

Chapter 6

Intermediate Silicon Layers (ISL)

6.1 Introduction

The SVX II silicon detector will provide coverage to $|\eta| \sim 2$. In the region $|\eta| < 1$ the combination of the SVX II and the Central Outer Tracker (COT) can provide full 3D tracking, but the reconstruction will need to be anchored on COT tracks, and suffer the multiplicative amplification of inefficiencies discussed in Chapter 3. For $|\eta| > 1$, SVX II can only perform 2D tracking and, in the absence of additional information, the impact parameter resolution for such tracks will be too poor to enable efficient b tagging.

Both of these problems are addressed by the Intermediate Silicon Layers (ISL): In the central region, a single layer of silicon is placed at a radius of 22 cm; six silicon based measurements in this region then provide a stand-alone segment for optimized tracking in conjunction with the COT. In the region $1.0 \leq |\eta| \leq 2.0$, where the COT coverage is incomplete or missing, two layers of silicon are placed at radii of 20 cm and 28 cm. Precision space point measurements at these radii will enable 3D track finding in the plug region and significantly improve the momentum resolution and, as a consequence, the impact parameter measurement. The ISL will thus extend tracking, lepton identification, and b-tagging capabilities over the full region $|\eta| \leq 2.0$.

6.2 Detector Design

6.2.1 Comparison to SVX II

The ISL incorporates many features of the SVX II design described in Chapter 5. For example, the two detectors are nearly identical with regard to:

- data acquisition
- power supplies

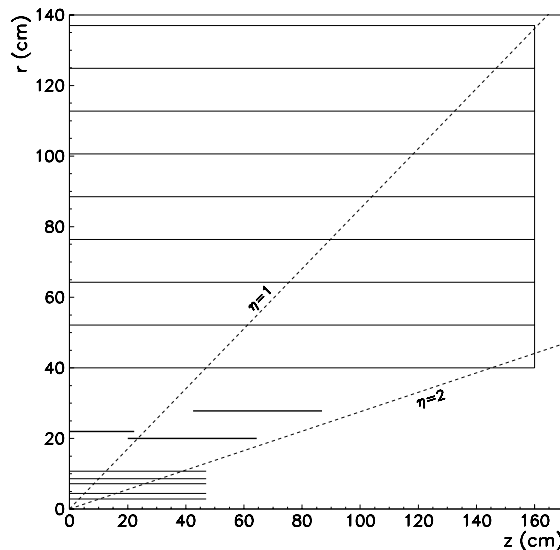


Figure 6.1: An r-z view of the ISL silicon layer placements. SVX II and COT are also shown.

- cooling system.

This overlap in designs has the obvious advantage of recycling much of the R&D that has already been done for SVX II.

However, there are several ways in which the ISL design differs from SVX II. In particular, the large surface area of silicon needed by the ISL necessitates cost saving simplifications. These can be achieved because many of the difficult tasks associated with the construction of a silicon microvertex detector are eliminated at larger radii. For example, since the occupancy is lower and radiation damage occurs more slowly, it is possible to use longer strips and wider readout pitch to reduce the number of readout channels and subsequent cost of front-end electronics and data acquisition. In addition, the intermediate radius region of CDF is rather spacious. This added

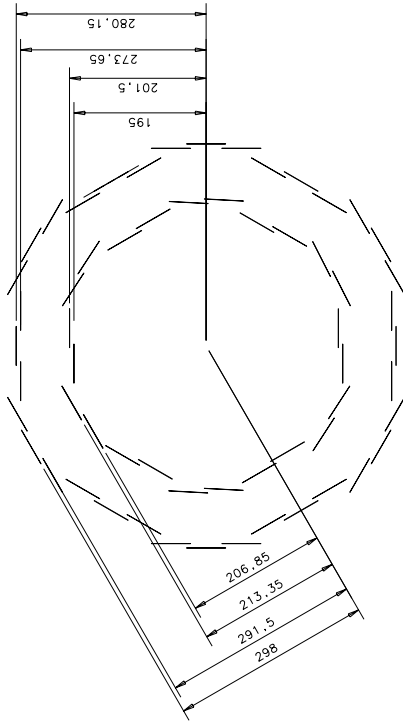


Figure 6.2: An r - ϕ view of the ISL silicon layer placements in the large η region.

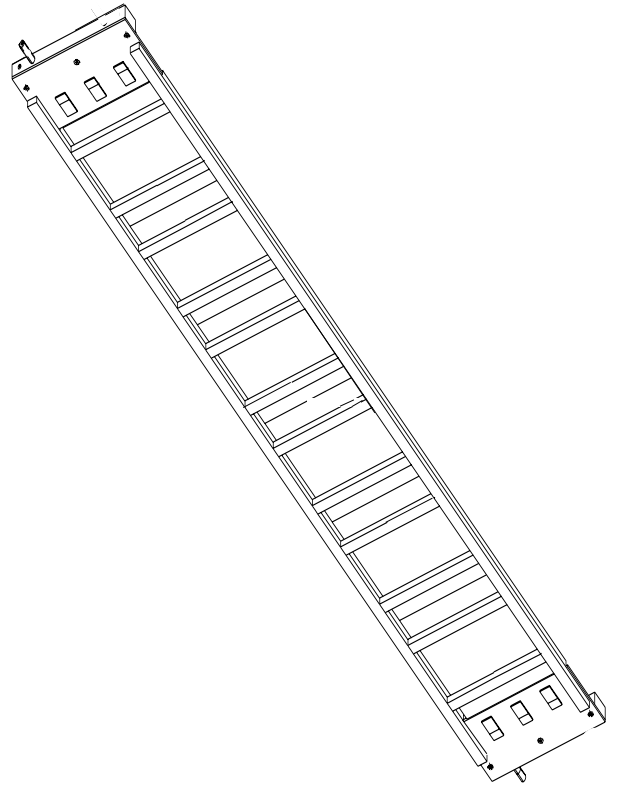


Figure 6.3: A view of the stereo side of a mechanical ladder which consists of two readout ladders.

real estate can be used to obtain a mechanical design for which the actual construction of the detector is more simple and robust while also less costly. Finally, since the layers are further from the interaction point, the construction tolerances are slightly more relaxed which again affords an opportunity to streamline the construction of the device.

6.2.2 Geometry

The positions of the silicon layers are shown in Figure 6.1. They lie within the radial range $20 < r < 30$ cm and extend to $|z| = 65$ cm for the inner layer and 87.5 cm for the outer layer ($|\eta| \sim 1.9$ in both cases). Figure 6.2 shows the end view of the two layers at large η .

6.2.3 Silicon Crystals

All silicon crystals used in ISL will be identical and measure 58 mm wide by 74 mm long; this is the largest size that still allows two crystals to be made on a single 6 inch Si wafer. As in layer 4 of SVX II, the crystals will be double-sided with axial strips on one side and small angle stereo strips on the other.

The stereo angle is 1.2° . The axial (p implant) side will have a strip pitch of $55 \mu\text{m}$. The stereo (n implant) side will have a strip pitch of $73 \mu\text{m}$. On both sides, the readout pitch will be twice the strip pitch to reduce the channel count. The intermediate strips will not be read out but will contribute to the resolution through charge sharing. The dimensions of the silicon crystals are summarized in Table 6.1. Several other experiments [1, 2] use silicon detectors with alternate strip readout. They are compared to the ISL design in Table 6.2.

6.2.4 Ladders

All ladders will be identical and will be made from 3 crystals laid end to end and microbonded to each other. The strips will be bonded to readout chips mounted on each side of a ceramic (alumina, AlN or BeO) readout hybrid. Four (three) SVX3 readout chips on the axial (stereo) side are matched to the detector strips by means of a pitch adapter. Figure 6.3 shows the stereo side of a mechanical ladder which is made up of two readout ladders containing 3 crystals each. Figure 6.4 shows close up views of the z and ϕ

	Atlas	Atlas	L3	L3	Delphi	Delphi	ISL	ISL
side	n	n	p	n	n	n	p	n
S/N	11	17	15	15	12	21	>12	12
RP (μm)	112	112	50	150	100	50	110	146
SP (μm)	56	56	25	50	100	50	55	73
SP/ $\sqrt{12}$	16.0	16	7.2	14.4	28.0	14.4	16.0	21.0
σ (μm)	15.6	12.9	7.0	15.0	23.0	10.0	<16.0	<23.0

Table 6.2: Comparison to other silicon detectors with alternate strip readout.

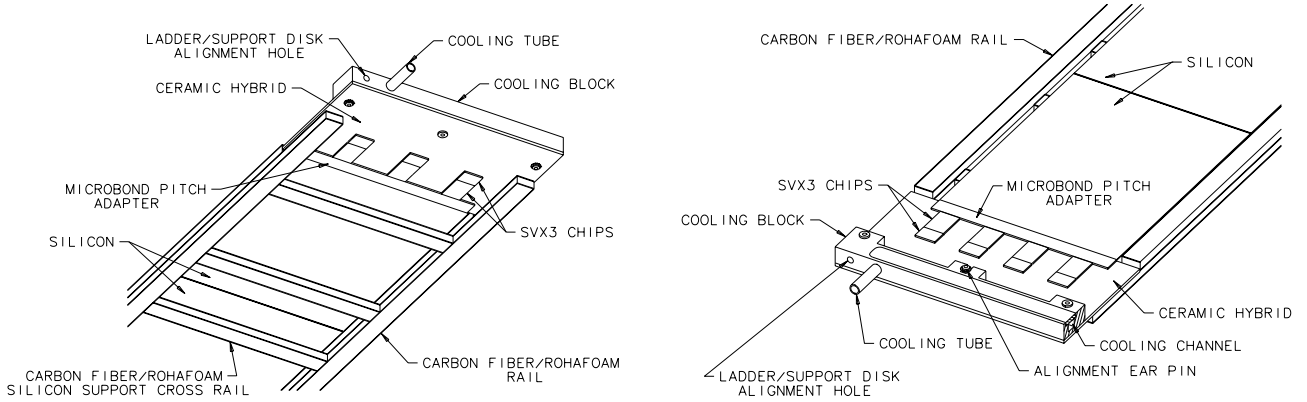


Figure 6.4: A close up view of the readout hybrid on the stereo side of a ladder (left) and the readout hybrid and cooling channel on the axial side of a ladder (right).

number of axial strips	1024
number of stereo strips	768
number of axial chips	4
number of stereo chips	3
stereo angle	1.2°
axial strip pitch (μm)	55
stereo strip pitch (μm)	73
axial readout pitch (μm)	110
stereo readout pitch (μm)	146
total width (mm)	58
total length (mm)	74
active width (mm)	56.3
active length (mm)	72.4

Table 6.1: ISL Sensor mechanical dimensions

readout segments. The ϕ side shows the attachment of the ceramic to a Be block by means of ‘ear-pins’ like those used to attach ladders to the Be bulkheads in the CDF SVX and SVX’ detectors. The Be block contains a water cooling channel; the entrance pipe is shown near the end of the block and the cover for the channel is seen on the top of the block. The size of the cooling channel is $3.5 \times 3.5\text{mm}^2$ which was determined to be adequate by comparison with the SVX II design.

An important design feature of the ladder is the positioning of the carbon fiber and foam support rails. As seen in the figure, the main support rails running the length of the ladder do not overlap any part of the silicon crystals. The crystals are instead supported by ‘rungs’ which bridge the main rails. This ‘outrigger’ design differs from the SVX II ladder design and results in open access to all bonding pads on both sides of the Si crystals.

Another difference from the SVX II design is that the readout hybrids are not glued to the silicon, but

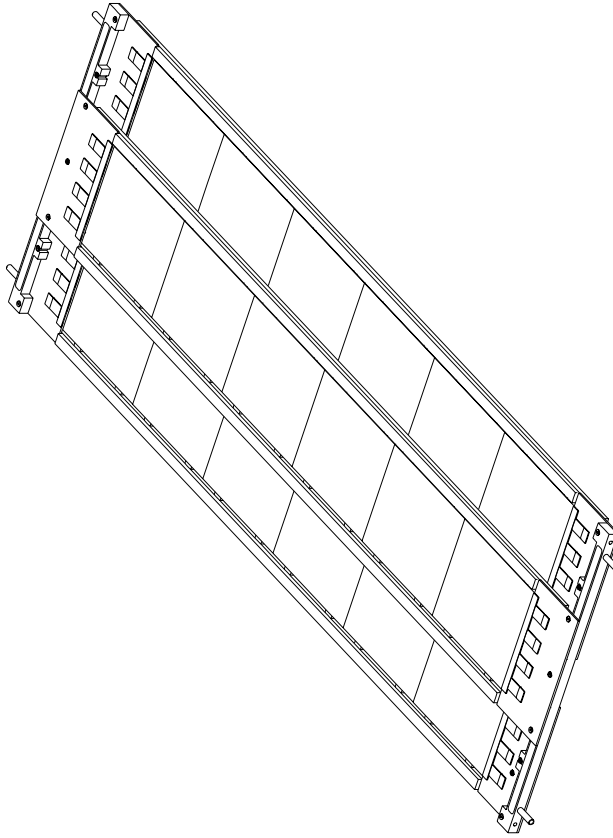


Figure 6.5: A view of a barrel 'slat' which consists of three ladders.

are placed at the ends as in the SVX and SVX' designs. Since the hybrids do not lie directly on the Si wafers, the transfer of heat to the Si is determined mainly by the thermal pathways provided by the microbond wires. Heating of the Si itself is less of a problem than for SVX II. These two features can be achieved without introducing dead areas in the layers by taking advantage of the large amount of space available. The result is a simple and robust ladder design.

6.2.5 Bulkheads

The ladders will be supported by carbon fiber disks. Note that in the largest radius layer, three ladders are attached to a single cooling channel per 30° wedge. A closeup is shown in Figure 6.6. The middle ladder is attached to one side of the block and the outer two are

on the opposite side as shown in Fig. 6.5. This allows adjacent ladders to be overlapped. The overlap is ~ 6 mm. For the inner radius layer two ladders are attached to the cooling block. This scheme results in a 30° wedge structure as for SVX II.

Figure 6.7 shows the basic layout of the carbon fiber support disks. Oblong channels allow the passage of cables. Smaller holes are shown for cooling pipes and attachment and alignment pins. A cross sectional view (r - z plane) of the ISL with offset layers is shown in Figure 6.8.

6.2.6 ISL mechanical support

6.2.6.1 Support structure specification

In order to allow $r - \phi$ pattern recognition within the SVX II and ISL system, the ISL readout strips must

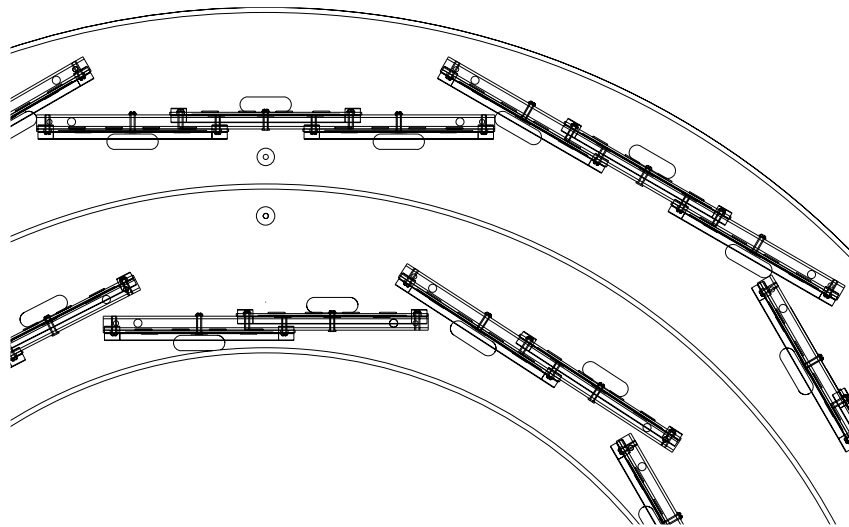


Figure 6.6: Closeup of one section of the end view of an endplug barrel.

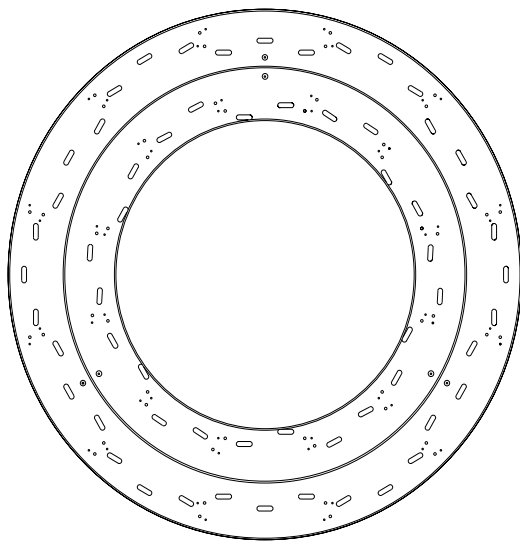


Figure 6.7: Carbon fiber support disks.

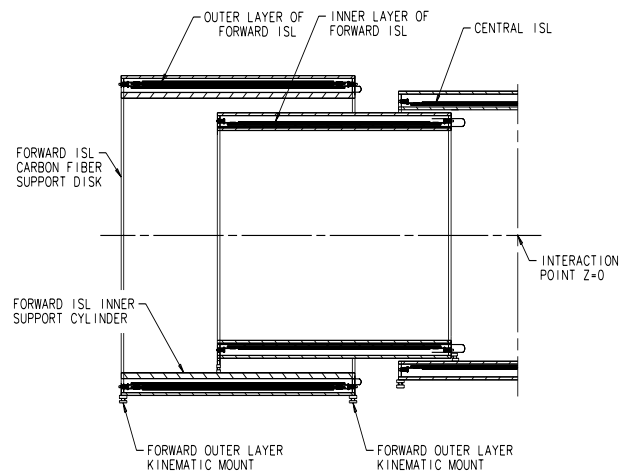


Figure 6.8: Schematic view of the ISL system.

be parallel to those of the SVX II within $\pm 200 \mu\text{m}$ over the length of the ISL ladder. Meeting this overall global specification requires that the axis of the ISL layers be aligned to within $\pm 180 \mu\text{m}$ of the SVX II axis over the length of an ISL layer. Such small alignment tolerances require that the layer positions be measured and adjusted on a precision coordinate measurement machine (CMM).

The ISL support structures provide a platform on which the layers can be mounted and surveyed using a CMM, and transfer the load of the layers to the COT endplates. In addition, the support system must carry the full mechanical load of the SVX II spaceframe assembly without compromising the precise alignment of the ISL. The system must also be stable against changes of temperature and humidity since the silicon detectors may require the circulation of cooled dry nitrogen to facilitate temperature regulation. Finally, the support system must introduce a minimum of material into the tracking volume in order to preserve the high precision of the tracking detectors.

6.2.6.2 ISL support system design

The main structural element of the ISL mechanical support system is a carbon fiber composite cylinder with an outer radius close to the inner radius of the COT. See Fig. 6.9. The large radius allows the construction of an extremely stiff tube with very little material. The cylinder consists of two carbon fiber skins separated by a honeycomb filler material. The Each carbon fiber layer is made of multiple plies of epoxy-impregnated carbon fibers, with the fibers in each oriented for maximum strength. The tube is kinematically supported at the ends by the COT endplates. Carbon fiber rings (“feedthrough flanges”) at the ends of the tube will prevent deformation of the cylinder under the load of the SVX II and ISL detectors.

Initially, the tube is constructed as two, independent half-cylinders. During the detector mounting procedure, the lower half-cylinder, without feedthrough flanges, will be placed in a fixture to maintain its shape as load is added. This configuration allows full access to the interior of the tube for the purpose of surveying detector positions. The central and outer ISL layers will then be kinematically mounted inside the lower half-cylinder and adjusted into position. Carbon fiber rings inside the tube will

distribute the point loads of the layers over the surface of the carbon fiber skins, thereby minimizing local deformations of the tube at the mount points. If the tube deflections under load are sufficiently small, then it should be possible to place the mounts with sufficient accuracy using a CMM to avoid the need for additional adjustments.

A third carbon fiber skin with a slightly smaller radius than the inner radius of the tube will be placed in the central part of the tube to provide a mounting platform for the central ISL.

After mounting the central and forward ISL layers, the inner layers will be kinematically mounted inside the outer layers. The load of the inner layers is first transferred to the inner surface of the outer layers, then to the ISL support cylinder through the outer layer support disks. Again, further adjustment of the layer positions may be unnecessary if the mounts can be placed with sufficient accuracy and the mounts do not move appreciably under load.

Cables and cooling pipes will be dressed along the sides of the lower half-cylinder. Additional non-structural hoops mounted to the lower half-cylinder outboard of the forward layers can be used to strain relieve cables and cooling tubes from the upper portion of the layers.

After ISL installation and alignment, the SVX II spaceframe/beam pipe assembly is inserted via a transfer fixture and kinematically mounted in the ISL. (The SVX II barrels are assumed to be mounted and properly aligned prior to this step.) Two choices are possible for the mount points of the SVX II spaceframe. In the first option, the load of the SVX II can be placed on the inner support cylinder of the outer forward ISL (as in Fig. 6.9). This load is then transferred from the forward ISL to the ISL support cylinder through the support disks of the outer layers. The second option completely removes the load from the ISL inner cylinder by extending the SVX II spaceframe to the ends of the outer forward layers. The load of the SVX II can then be transferred directly through the ISL support disks to the ISL support cylinder. Lengthening the SVX II spaceframe without altering the basic design will increase the expected sag of the SVX II frame to $12 \mu\text{m}$, compared to $7 \mu\text{m}$ for the shorter design. The larger value is well within the design specifications for the SVX II spaceframe. In either option, it should be possible to position the mounts for the SVX II spaceframe with sufficient precision that further adjustment of

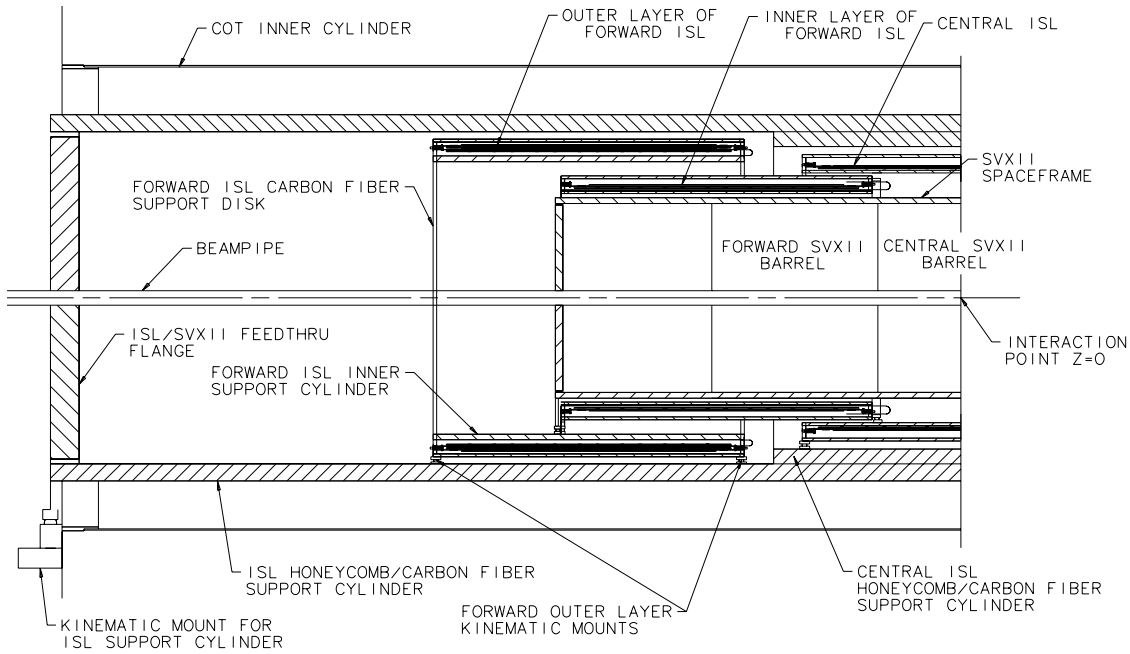


Figure 6.9: An r-z view of the ISL spaceframe support system.

the SVX II position is unnecessary.

The final steps in the assembly of the ISL support cylinder require mounting the top half-cylinder to the bottom half-cylinder and installing the feedthrough flanges to strengthen the ends of the completed tube. In order to preserve the alignment of the various detectors, this procedure may introduce no new internal stresses. A similar problem exists in SVX II for joining the bulkheads into a single barrel after all ladders have been installed, and has been successfully used during SVX and SVX' construction. After joining the two half-cylinders, the beam pipe load will be transferred to the ISL support cylinder, and the feedthrough flanges installed and glued into place. Slots in the feedthrough flanges permit cables and cooling pipes to exit the tracking volume.

6.3 Readout and Data Acquisition

SVX3 readout chips are used so that the data acquisition (DAQ) system is identical to the SVX II system described in Chapter 5. However, the low occupancy of ISL allows a coarser DAQ segmentation to reduce the size and cost of the system. Two ladders will be attached to each portcard input so that a single port-

	SVX II	ISL
Detectors	720	900
Half ladders	360	300
Chips	3168	2100
Channels	405,504	268,800
Hybrids	720	300
Port Cards	72	30

Table 6.3: Comparison of component counts in SVX II and ISL.

card covers two 30° wedges. This assigns about 60% more channels to each portcard than is done in SVX II, but the readout time will be less than SVX II since less $\eta\phi$ space is covered by each portcard input. The component count for the ISL is compared to SVX II in Table 6.3. Notice that the ISL uses more silicon than SVX II, but it has about half as many channels and portcards.

The cabling is also copied from the SVX II design. The space required to route cables from the port cards to the FIBs outside the detector volume is expected to be about 25 of the 250 available slots.

6.4 ISL Performance Issues

We address here a number of performance concerns which are close to the hardware: occupancy, signal-to-noise ratio, material, and hit resolution. We also show with a simple calculation that the ISL acceptance for tracks already in the SVX II is very high, which is crucial if the SVX II + ISL are to function as a single “inner tracker”. A simulation study of the performance of the ISL in the CDF II “integrated tracking” environment is presented in Chapter 7.

6.4.1 Hit Occupancy

The large radius of the ISL leads to very low occupancies. Based on a measurement from SVX’ data in minimum bias triggers, the expected occupancy from a single minimum bias interaction is only 0.08%. For a $t\bar{t}$ event at $\mathcal{L} = 2 \times 10^{32} \text{cm}^{-2} \text{s}^{-1}$ @ 396 ns, the occupancy predicted from Monte Carlo is 0.7%. This low occupancy is a significant advantage for the pattern recognition.

6.4.2 Signal to Noise

Each ISL ladder contains three silicon crystals while SVX II ladders are made from two. The extra ladder length reduces the channel count, but it also increases the capacitance that loads the front end amplifier by about 50% to 30 pF for the axial side and 40 pF for the stereo side. The increased capacitance results in a larger RMS noise. From Fig. 5.5 in Chapter 5, the expected noise at 396 ns bunch crossing (371 ns integration time) is $1300e^-$ for the axial side and $1700e^-$ for the stereo side. For 132 ns bunch crossing (107 ns integration time), the noise increases to $2200e^-$ for the axial side and $3000e^-$ for the stereo side. In the worst case, the signal to noise is $\sim 8:1$. Monte Carlo studies and experience with SVX’ have shown no significant deterioration in hit finding at signal to noise values as low as $\sim 4:1$. The low radiation dose expected at the ISL radii reduces the need to begin with a higher signal to noise.

6.4.3 Material

The material contributed by each ISL ladder is similar to an SVX II ladder. In the central region, the single ISL layer amounts to $\sim 0.5\%$ of a radiation length (at 90° incidence). The two layers in the plug region amount to $\sim 1\%$. The additional material from the

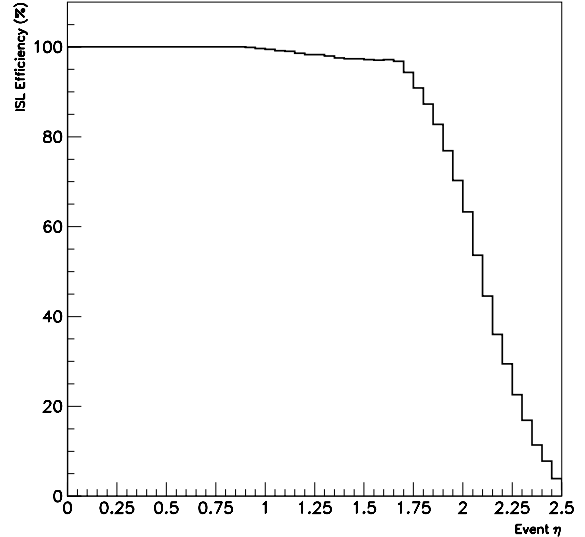


Figure 6.10: ISL acceptance for tracks which are contained within SVX II.

hybrids, bulkheads, portcards, etc., amounts to an additional 1% when averaged over the length of the detector. The total material is then $\sim 2\%$ of a radiation length.

6.4.4 Hit resolution

The readout pitch is twice the strip pitch. By using charge sharing to interpolate the track impact position, the axial hit resolution is expected to be $\leq 16 \mu\text{m}$. Similarly, the stereo hit resolution is expected to be $\leq 23 \mu\text{m}$ perpendicular to the strip direction. Of course, the alignment and construction tolerances are important to the final resolution as discussed below.

6.4.5 Acceptance

Since there is ample space in the intermediate region, the ladders are staggered in radius and in z to eliminate gaps. The overlap between adjacent ladders is $\sim 6 \text{mm}$ in $r - \phi$ to account for the insensitive regions on the stereo side. The acceptance is then dominated by the length of the detector, which extends to $|\eta| \sim 1.9$ (see Fig. 6.1). We have performed a simple simulation to calculate the ISL acceptance for particles already contained within SVX II, for the case of an extended luminous region with $\sigma_z = 30 \text{cm}$. The result, Fig. 6.10, shows that even with a long bunch, the ISL will record over 95% of the par-

ticles seen by the SVX II out to event $|\eta|=1.7$, and is still 50% efficient for tracks at $|\eta|=2.0$.

6.5 Construction Tolerances

The most crucial aspect of the construction of the detector is the ladder internal alignment. By this we mean the alignment of strips from wafer to wafer and the referencing of the strips to the ear-pin holes on the readout hybrid. Ideally one would like this alignment to be better than the intrinsic hit resolution of the sensors. Fortunately the construction of the ladder is carried out with a precision coordinate measuring machine (CMM) having typical resolution of 0.1-0.2 mil (2.5-5.0 μm) using positioning fixtures like those used in the SVX and SVX' projects. In these projects, the ladder internal alignments that were achieved were consistent with the CMM resolution.

Ladder to ladder alignments in a given layer, from layer to layer, and relative to the SVX II ladders are important for the pattern recognition but do not necessarily limit the final resolution of the device. In particular, it is anticipated that the ladders will be aligned using tracks which traverse the COT and SVX II. Thus, given that the ladders are themselves very precisely constructed, it should be possible to locate them and determine alignment constants that describe how their positions deviate from nominal. This will insure that hit resolution is not degraded for those cases in which the z locations of the axial hits are known. The z position is necessary in order to remove $r - \phi$ displacements resulting from strips not being parallel to those in SVX II. We have chosen $\pm 75 \mu m$ as our specification for tolerable $r - \phi$ ladder-to-ladder misalignment (in a single layer) to insure the convergence of the alignment procedure. As discussed below, the actual misalignments are expected to be about half this amount.

If the pattern recognition relies on starting from axial-only reconstruction of tracks in Si layers, then the z location of axial hits will not yet be known and the actual relative misalignments of ladders will contribute an $r - \phi$ uncertainty which could be large. Ideally, you want the maximum $r - \phi$ deflection relative to SVX II ladders to be less than the two hit resolution ($\sigma = 220 \mu m$) and less than the $r - \phi$ pointing resolution from SVX II ($\sigma = 250 \mu m$). It can be shown that this means that the deflection angle $\delta\alpha$ which measures the degree to which the strips in an

	Necessary	Achievable
Wafer-to-Wafer	$\pm 5 \mu m$	$\pm 2.5 \mu m$
Wafer-to-Hybrid	$\pm 5 \mu m$	$\pm 2.5 \mu m$
Hybrid-to-Block	$\pm 25 \mu m$	$\pm 13 \mu m$
Block-to-Disk	$\pm 50 \mu m$	$\pm 25 \mu m$
Ladder-to-Ladder	$\pm 75 \mu m$	$\pm 40 \mu m$
ISL-to-SVX II	$\pm 200 \mu m$	$\pm 100 \mu m$

Table 6.4: Summary of the necessary and achievable ISL construction tolerances.

outer layer are not parallel to those in SVX II, should satisfy

$$\delta\alpha < \frac{2\sigma}{L(1.5 + \frac{3.0}{\sqrt{12}})} = 0.4 \text{ mrad}$$

Note that this corresponds to 8 mil across the $L \sim 50$ cm length of the barrel. As described above, it is our plan to build the intermediate radius Si layers and then assemble them together with the SVX II using a large CMM for alignment. This will allow the relative angle between the axis of SVX II and that of the ISL layers to be kept to $\delta\alpha < 0.2$ mrad. This is adequate to allow axial-only tracking provided the ladder to ladder alignment in the ISL is not itself worse than 8 mil.

The ladder to ladder $r - \phi$ alignment within the ISL is determined by several factors. First, the alignment of the hybrid connection holes to the pin holes on the cooling block which attach the ladder to the carbon fiber support disk will introduce an uncertainty of no more than 0.5 mil at each hybrid. The alignment of the Be block to the carbon fiber support disk is dominated by the reference hole positioning and clearance. This can be achieved with an uncertainty of less than 1.0 mil at each end. Taking the conservative estimate for the ladder internal alignment to be $\pm 10 \mu m$, it then follows that the ladder to ladder alignment in a single layer will be

$$\sigma < \sqrt{2 \cdot (10^2 + 13^2 + 25^2)} \sim 40 \mu m$$

Layer to layer alignment will contribute an additional global uncertainty of 25-50 μm which however will not seriously impact tracking alignment or ultimate performance of the detector. We conclude that the design we have presented will allow construction within the tolerances necessary for the success of the

axial-only stage of the pattern recognition and for the alignment and full resolving power of the detectors in 3D tracking. A summary of the necessary and achievable tolerances is contained in Table 6.4.

Bibliography

- [1] P. Weilhammer "Double-sided Si strip sensors for LEP vertex detectors" Nucl.Instr. and Meth. A 342 (1994) 1
- [2] P.P. Allport et al. "Performance of the ATLAS-A silicon detectors with analogue readout" ATLAS-INDET-NO-133 (1996)